

# **Computational Study of Nonlinear Plasma Waves:**

## **I. Simulation Model and Monochromatic Wave Propagation**

by

**Y. Matsuda and F. W. Crawford**

(NASA-CR-142020) COMPUTATIONAL STUDY OF  
NONLINEAR PLASMA WAVES: 1: SIMULATION  
MODEL AND MONOCHROMATIC WAVE PROPAGATION  
(Stanford Univ.) 40 p HC \$3.75 CSDL 201  
N75-16348  
Unclas  
G3/75 07759

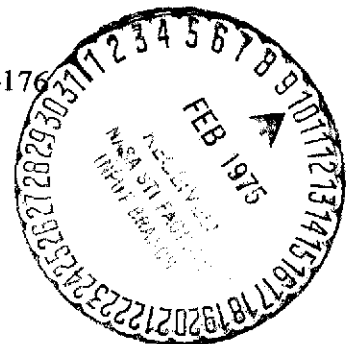
**December 1974**

**SU-IPR Report No. 607**

NSF Grant GP 43703X

and

NASA Grant NGL 05-020-176



**INSTITUTE FOR PLASMA RESEARCH  
STANFORD UNIVERSITY, STANFORD, CALIFORNIA**

COMPUTATIONAL STUDY OF NONLINEAR PLASMA WAVES:

I. SIMULATION MODEL AND MONOCHROMATIC WAVE PROPAGATION

by

Y. Matsuda and F. W. Crawford

NSF Grant GP 43703X

and

NASA Grant NGL 05-020-176

SU-IPR Report No. 607

December 1974

Institute for Plasma Research  
Stanford University  
Stanford, California 94305

# COMPUTATIONAL STUDY OF NONLINEAR PLASMA WAVES:

## I. SIMULATION MODEL AND MONOCHROMATIC WAVE PROPAGATION<sup>\*</sup>

Y. Matsuda<sup>†</sup> and F. W. Crawford

Institute for Plasma Research  
Stanford University  
Stanford, California 94305

### ABSTRACT

In this paper, an economical low-noise plasma simulation model originated by Denavit is applied to a series of problems associated with electrostatic wave propagation in a one-dimensional, collisionless, Maxwellian plasma, in the absence of magnetic field. In Part I, the model is described and tested, first in the absence of an applied signal, and then with a small amplitude perturbation. These tests serve to establish the low-noise features of the model, and to verify the theoretical linear dispersion relation at wave energy levels as low as  $10^{-6}$  of the plasma thermal energy: better quantitative results are obtained, for comparable computing time, than can be obtained by conventional particle simulation models, or direct solution of the Vlasov equation. The method is then used to study propagation of an essentially monochromatic plane wave. Results on amplitude oscillation and nonlinear frequency shift are compared with available theories. The additional phenomena of sideband instability and satellite growth, stimulated by large amplitude wave propagation and the resulting particle trapping, are described in Part II.

---

<sup>\*</sup>This work was supported by the National Aeronautics and Space Administration, and the National Science Foundation.

<sup>†</sup>Now at Plasma Physics Laboratory, Princeton University, Princeton, N.J. 08540.

## CONTENTS

|   | <u>Page</u> |
|---|-------------|
| ABSTRACT . . . . .                            | ii          |
| 1. INTRODUCTION . . . . .                     | 1           |
| 2. HYBRID SIMULATION MODEL . . . . .          | 3           |
| 2.1 Quiet Start . . . . .                     | 5           |
| 2.2 Periodic Smoothing . . . . .              | 6           |
| 2.3 Comparison with Denavit's Model . . . . . | 7           |
| 3. EQUILIBRIUM BEHAVIOR . . . . .             | 9           |
| 4. LINEAR WAVE PROPAGATION . . . . .          | 13          |
| 4.1 Recurrence Phenomenon . . . . .           | 15          |
| 5. NONLINEAR WAVE PROPAGATION . . . . .       | 18          |
| 5.1 Computations . . . . .                    | 21          |
| 5.2 Comparison with Theory . . . . .          | 26          |
| 6. DISCUSSION . . . . .                       | 33          |
| REFERENCES . . . . .                          | 35          |

# FIGURES

|   | <u>Page</u> |
|---|-------------|
| 1. Phase-space covered with a rectangular grid, and a Maxwellian velocity distribution approximated by beams. . . . .   | 4           |
| 2. Equilibrium behavior for various values of $N_s$ . [ $\Delta v = v_t/7$ , $N = 2048$ , $L = 32 \Delta x$ , particle size $H = \Delta x = \lambda_D$ , $v_1 = -4.5 v_t$ , $v_2 = 4.5 v_t$ , $\Delta t = 0.25/\omega_p$ ] . . . . .  | 10          |
| 3. Time-averaged energy spectrum of the system shown in Fig. 2. . .   | 11          |
| 4. Simulation of Landau damping. Solid lines are the prediction of the Langdon theory <sup>6</sup> . Dashed line is the prediction of point particle theory. . . . .  | 14          |
| 5. Linear wave dispersion. Simulation results are shown by circles and bars whose sizes indicate errors involved. [ $\Delta v = v_t/7$ , $N_s = 16$ , $N = 8192$ , $L = 128 \Delta x$ , $v_1 = -4.5 v_t$ , $v_2 = 4.5 v_t$ , $\Delta t = 0.25/\omega_p$ ] . . . . .   | 16          |
| 6. Amplitude oscillation of a large amplitude monochromatic wave. [ $\Delta v = v_t/14$ , $N_s = 16$ , $N = 8192$ , $L = 64 \Delta x$ , $H = \Delta x = \lambda_D$ , $v_1 = -4.25 v_t$ , $v_2 = 4.82 v_t$ , $\Delta t = 0.25/\omega_p$ ] (Nonsymmetric velocity-space is used to provide resonant particles at high velocities) . . . . . | 22          |
| 7. Temporal behavior of the spatially averaged distribution function in the simulation shown in Fig. 6. The phase velocity of the wave is marked by an arrow . . . . .  | 24          |
| 8. Temporal evolution of amplitude for various initial amplitudes, i.e., $\gamma_L/\omega_B$ . . . . .  | 25          |
| 9. Nonlinear frequency shift of an electron plasma wave. [ $\Delta v = v_t/7$ , $N_s = 16$ , $N = 4096$ , $L = 50 \lambda_D$ , $H = \Delta x = (50/64)\lambda_D$ , $v_1 = -3.79 v_t$ , $v_2 = 5.21 v_t$ , $\Delta t = 0.25/\omega_p$ ] . . . . .  | 27          |

## 1. INTRODUCTION

This paper is concerned with computer simulation of electron plasma waves in a Maxwellian plasma, in the absence of magnetic field. The aims of our simulations are, first, to develop an economical low-noise simulation technique, and second, to apply it to the study of linear and non-linear wave phenomena in a one-dimensional plasma with periodic boundary conditions. Throughout the work, emphasis is placed on simulations for wave and plasma parameters comparable with those assumed in available theories, and accessible in laboratory experiments.

There are two distinctly different approaches to the simulation of plasma dynamics: first is the use of a particle simulation model in which individual charged particles are followed, and second is direct numerical solution of the Vlasov equation describing the charged particle velocity distribution function. The particle simulation model has the disadvantage that the fluctuation level is usually several orders of magnitude higher than in an actual plasma. This stems from the fact that it is not feasible to follow on the computer the dynamics of as many particles as there are in a plasma. The fluctuations not only give rise to non-physical effects, but also make it difficult to study linear and weakly nonlinear phenomena. This is particularly unfortunate since most of the nonlinear theories to date are based on an expansion method which is valid only in weakly nonlinear cases. Consequently, they cannot be clearly validated by particle simulation, nor vice versa. Direct solution of the Vlasov equation is subject to numerical instability associated with the free-streaming term in the Vlasov equation. This tends to limit application

of the method to short-time simulations. However, since the Vlasov equation does not contain discrete particle encounters and thermal fluctuations of macroscopic quantities such as the electric field and charged particle density, the behavior of very small amplitude waves can be studied in a quantitatively accurate manner.

Denavit has proposed a hybrid approach which can drastically reduce the fluctuations inherent in the particle simulation model, and greatly ease the computational difficulties of the Vlasov equation approach.<sup>1</sup> His model is a particle simulation model in the sense that the motions of a large number of particles are followed in time. The particles do not keep their identities, however, and there are similarities to the Vlasov approach in that values of the velocity distribution function are defined on a grid in phase-space. Despite its attractive features, and obvious potential for application to a wide range of linear and nonlinear problems, little use of the approach seems to have been made so far. The purpose of this paper is to apply it to a logical series of such problems, involving electron plasma waves in a Maxwellian plasma, and so provide results for quantitative comparison with available theories and experimental results.

In Section 2, a hybrid simulation model suitable for studying one-dimensional electron plasma waves is described. In Section 3, its equilibrium characteristics are tested, i.e., noise growth with zero applied signal amplitude is examined. In Section 4, linear wave propagation is studied, for a very small amplitude monochromatic signal. Progressive increase in signal amplitude causes amplitude oscillation, nonlinear Landau damping, and nonlinear frequency shift effects to appear. These phenomena are studied in Section 5. The results are discussed briefly in Section 6.

## 2. HYBRID SIMULATION MODEL

The model to be used in this work employs a cloud-in-cell (CIC) scheme. This was originally devised to reduce fluctuations in particle simulation models, and involves considering the particles as clouds of distributed charge; the center of the cloud is taken to be the particle coordinate, and a spatial grid is used for computing field quantities.<sup>2</sup> In addition to this grid, we introduce a grid in velocity-space, and represent the particles by points in  $(x-v)$  phase-space as shown in Fig. 1. The phase-space is consequently covered with a rectangular grid of dimensions  $\Delta x, \Delta v$ . The velocity grid extends from  $v_1$  to  $v_2$ , where  $v_1$  and  $v_2$  are chosen such that the numbers of particles with velocities in the intervals  $v < v_1$  or  $v > v_2$  are negligible.

In creating a plasma with a Maxwellian velocity distribution, our model employs the following method. The particles are equally divided into a number of velocity groups. All the particles in one group are assumed to have the same velocity,  $v$ , and mass and charge are assigned to them in proportion to  $\exp(-v^2/2v_t^2)$ , where  $v_t$  is the electron thermal velocity. This is shown schematically in Fig. 1. Since the charge-to-mass ratio is the same for all of the particles, the acceleration is also the same. One of the advantages of this method of generating a Maxwellian distribution by weighted particles is that improved resolution is provided in the tail of the velocity distribution, compared with a Maxwellian distribution with identical particles.

The system is set up at time  $t = 0$  using a quiet start technique, and proceeds as in a CIC model. After a certain number of time-steps,



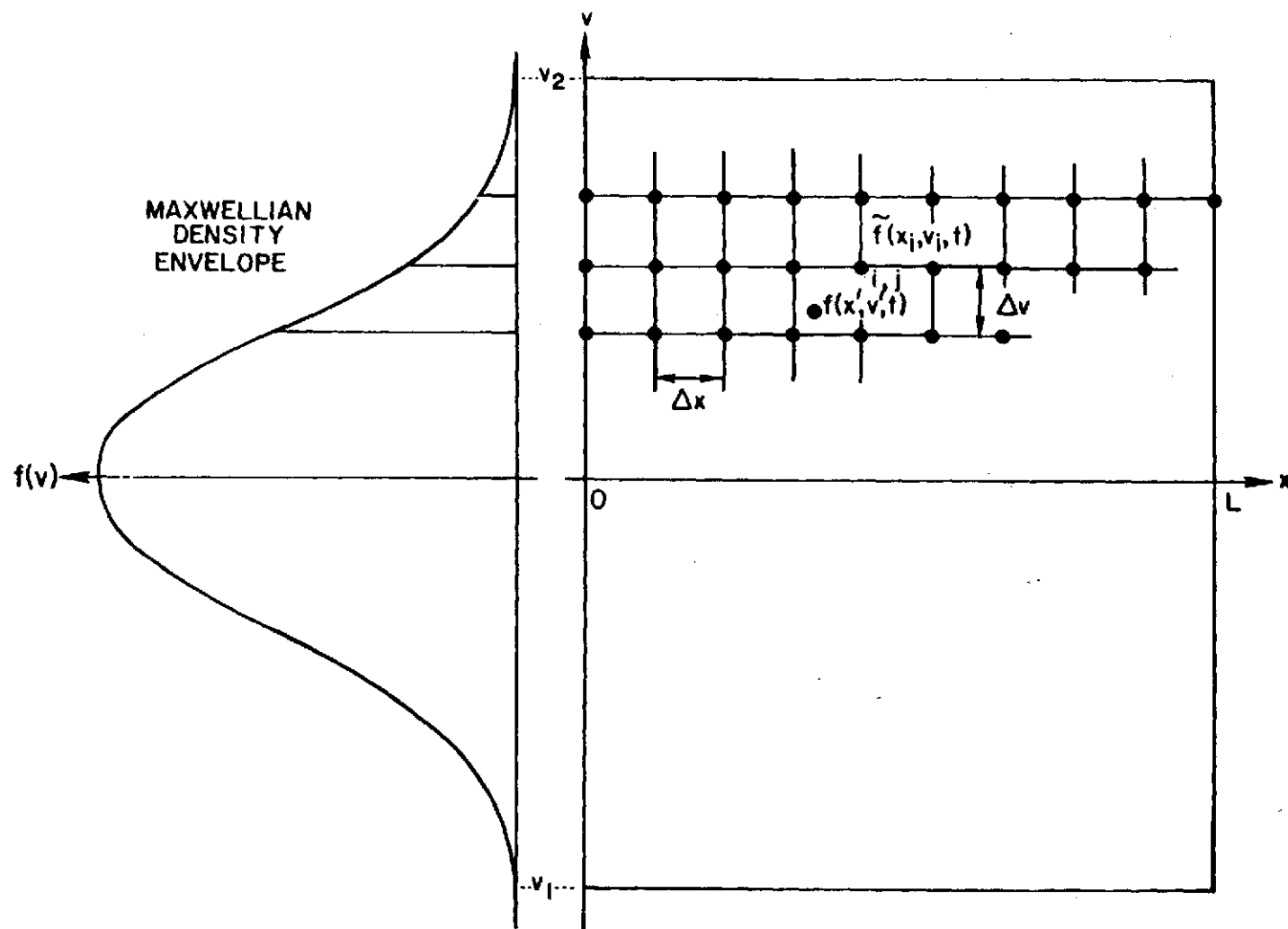


FIG. 1. Phase-space covered with a rectangular grid, and a Maxwellian velocity distribution approximated by beams.

the distribution function is reconstructed at the grid points by periodic smoothing, and is interpreted as representing a distribution of new discrete particles. The motions of these particles are followed until the next reconstruction. The quiet start technique, and the periodic smoothing, are essential parts of the hybrid approach proposed by Denavit. They are used to achieve a very low fluctuation level, and allow the model to be applied to a wide range of linear and nonlinear problems.

## 2.1 Quiet Start

The quiet start technique, proposed by Byers, is a method of eliminating macroscopic fluctuations in a particle code at early stages of evolution.<sup>3</sup> This is done by placing the particles only on the equilibrium trajectories in phase-space at time  $t = 0$ , as shown in Fig. 1, and in principle provides a noiseless system. In practice, round-off errors due to the finite number of digits representing the numbers in the computer introduce some fluctuations. However, this level is many orders of magnitude lower than that in the particle codes.

Although the quiet start technique works well at early times, it ceases to be effective after a time,  $2\pi/(k_m \Delta v)$ , where  $k_m$  is the maximum wavenumber possible in the system.<sup>1</sup> This breakdown occurs because the velocity distribution of the particles is being replaced by a set of discrete beams. Such a system is also subject to streaming instability, even if the envelope of the beam density is Maxwellian.<sup>4</sup> In the limit of small beam spacing, the temporal growth rate,  $\omega_i$ , is given by<sup>1</sup>

$$\omega_i \approx \frac{k\Delta v}{2\pi} \left| \ln \left( \frac{\Delta v}{v_t} \right) \right| \quad \left( \frac{\Delta v}{v_t} \rightarrow 0 \right) . \quad (1)$$

Therefore, a simulation can be carried out with very low fluctuations up to times of order  $\omega_i^{-1}$ . Since  $\omega_i \rightarrow 0$  as  $\Delta v \rightarrow 0$ , in principle it is possible to perform a low-noise simulation for as long as is desired by choosing a sufficiently small  $\Delta v$ . In practice, however,  $\Delta v$  cannot always be made as small as is desirable, because the smaller  $\Delta v$  is to be, the more particles are necessary. Periodic smoothing may be used to combat this instability, and to make a long-time simulation possible with a relatively small number of beams.<sup>1</sup>

## 2.2 Periodic Smoothing

Periodic smoothing constitutes a periodic averaging of the distribution function in phase-space. It can be expressed by

$$\tilde{f}(x, v, t) = \iint f(x', v', t) w_x(x - x') w_v(v - v') dx' dv' , \quad (2)$$

where  $w_x$  and  $w_v$  are weighting functions for coordinate- and velocity-space,  $\tilde{f}$  is the averaged distribution function, and the integration is over the whole of phase-space.

In particle models with a phase-space grid such as that shown in Fig. 1, the integral in Eq. (2) reduces to a sum over the collection of particles, and we want to find the averaged distribution function,  $\tilde{f}$ , at the phase-space grid points. If  $f(x', v', t)$  is taken to be the mass of a finite-size particle, the center of which is located at  $(x', v')$  at time  $t$ , then Eq. (2) implies that the value of  $\tilde{f}$  at the  $(i-j)$  grid point,  $(x_i, v_j)$ , is obtained by distributing the mass of each particle among the neighboring grid points according to the weighting prescribed by  $w_x$  and  $w_v$ . This is a reconstruction of the distribution function from a given distribution of particles.

Since the smoothing process expressed by Eq. (2) does not conserve all of the moments of the distribution function, it causes diffusion of the distribution function. It is to be expected that, with judiciously chosen weighting functions, this diffusion may suppress the streaming instability with a minimum of other undesirable effects. Such weighting functions are described, and their diffusion rates are estimated, in Reference 1. In our work, we shall use the quadratic weighting function which conserves particles, momentum, and energy. The frequency of smoothing necessary to quench the streaming instability depends on the choice of weighting function and the beam spacing. A rough estimate would be that at least one smoothing operation is necessary within the growth time of a perturbation with the maximum wavenumber of the system.

### 2.3 Comparison with Denavit's Model

In the work of Denavit,<sup>1</sup> the Lewis variational method<sup>5</sup> was used to construct a model. In the Denavit model, finite-size particles are chosen to have a triangular spatial distribution, instead of the uniform charge distribution of the CIC model. The numerical scheme based on that model turned out to be more complicated, therefore more time-consuming, than our model. In addition, although his scheme is energy-conserving, it does not conserve momentum, whereas the CIC scheme is formulated in such a way as to conserve momentum.<sup>6</sup> The non-conservation of momentum indicates the existence of self-force, i.e., a particle is effected by the force due to the field that is created by itself, which is non-physical. The energy-conserving feature of the Denavit scheme may not be very useful in practice, since energy conservation is exact only in the limit of a vanishingly small time-step.

It may be remarked, further, that in testing his model Denavit chose to study two-stream instability. He compared his results with those from a particle code<sup>7-9</sup> and the Vlasov approach.<sup>9</sup> These simulations were carried out at relatively high electrostatic energy levels, i.e.,  $10^{-3} - 10^{-2}$  times the total energy, which is to be compared with an order of  $10^{-6}$  in our tests to be described in Section 4.

### 3. EQUILIBRIUM BEHAVIOR

It is logical to begin our series of numerical experiments on a Maxwellian plasma with no applied perturbation at all. Here, and throughout the paper, only electron motions are followed; positive ions are considered to constitute a homogeneous, immobile, neutralizing background. Periodic boundary conditions are applied in space: a particle leaving one end of the system is immediately reintroduced at the other with the same velocity. The most important parameters are the number of time-steps,  $N_s$ , after which the smoothing operation is repeated, and the beam spacing,  $\Delta v$ .

In Fig. 2, the total field energy is plotted against time for  $\Delta v = v_t/7$ . It will be seen that by increasing the frequency of smoothing, i.e., decreasing  $N_s$ , the streaming instability is suppressed; for  $N_s \leq 32$ , the field energy stays roughly constant throughout the simulation run. To study this further, the initial energy spectrum, and the time-averaged energy spectrum are shown in Fig. 3. The energy spectrum for  $N_s = 32$  shows that mode energy tends to increase as time increases. For  $N_s = 16$  and 8, the mode energy seems to stay at roughly the same level, i.e., the streaming instability is stabilized. The total energy of the system, i.e., the particle kinetic energy plus the field energy, was found to be conserved to within 0.1% up to  $\omega_p t \simeq 270$ , where  $\omega_p$  is the electron plasma frequency.

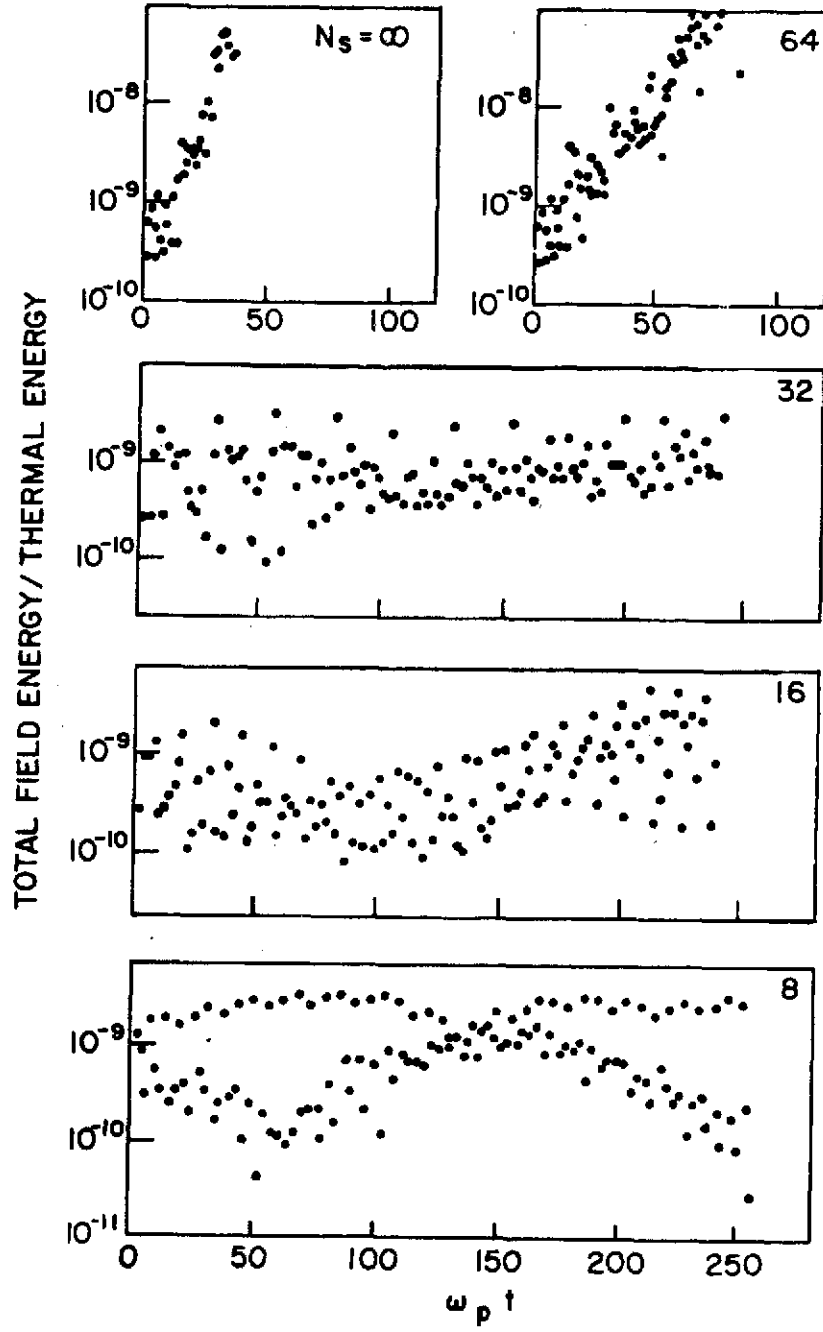


FIG. 2. Equilibrium behavior for various values of  $N_s$ . [ $\Delta v = v_t/7$ ,  $N = 2048$ ,  $L = 32 \Delta x$ , particle size  $H = \Delta x = \lambda_D$ ,  $v_1 = -4.5 v_t$ ,  $v_2 = 4.5 v_t$ ,  $\Delta t = 0.25/\omega_p$ ].

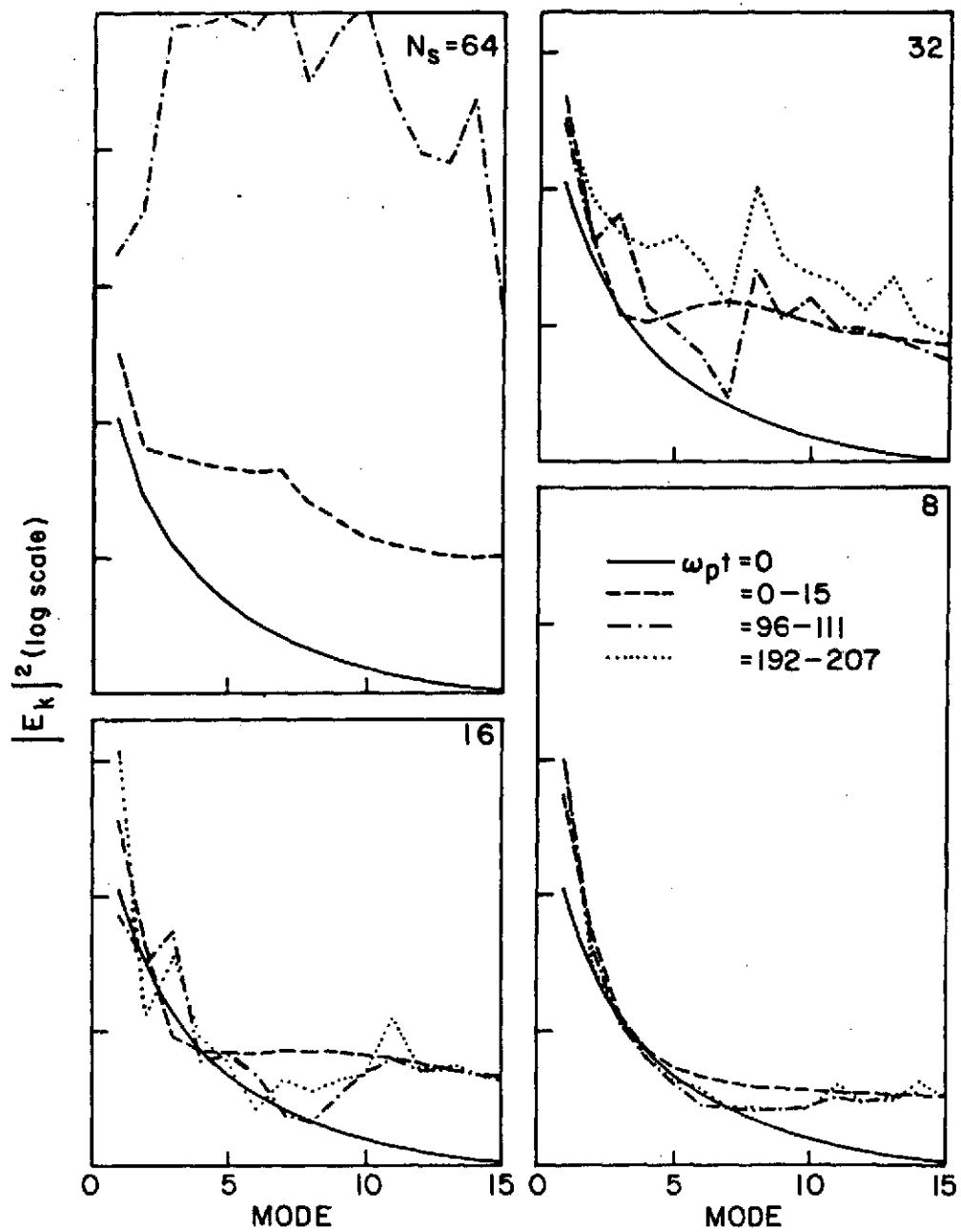


FIG. 3. Time-averaged energy spectrum of the system shown in Fig. 2.



In a simulation for  $\Delta v = v_t/14$  , it was observed that the growth rate of the field energy is greatly reduced compared with the case  $\Delta v = v_t/7$  , and larger values of  $N_s$  are adequate to suppress the streaming instability.<sup>10</sup>

The important fact established here is that, for stable cases, the total field energy is fluctuating at a level  $10^{-8}$  times lower than the thermal energy of the plasma during the whole run. Since the level of fluctuations in the particle model for a system of length  $L = 32 \lambda_D$  , where  $\lambda_D$  is the electronic Debye length, with  $N = 4096$  electrons, is of the order of  $10^{-3} - 10^{-2}$  times the thermal energy, we have achieved 50 - 60 dB reduction in fluctuations. The fluctuation amplitude in the particle model can be reduced by increasing  $N$  , but it should be remembered that the level varies only as  $N^{-1/2}$  .

#### 4. LINEAR WAVE PROPAGATION

The purpose of this simulation was to verify predictions of Landau damping for electron plasma waves. Waves were excited at  $t = 0$  by applying the perturbations

$$\Delta x_i = \Lambda_D \cos kx_i, \quad \Delta v_i = \Lambda v_t \sin kx_i, \quad (3)$$

where  $x_i$ ,  $\Delta x_i$ , and  $\Delta v_i$  are the position, displacement, and velocity perturbation of particle  $i$ ,  $\Lambda$  is the amplitude, and  $k [= 2\pi/L]$  is the wavenumber. In this simulation, only Mode 2 ( $n = 2$ , i.e., there are two wavelengths in the system) was excited. The results are shown in Fig. 4. For  $N_s \leq 16$ , there is excellent agreement with the theoretical prediction by Langdon,<sup>6</sup> shown by solid lines, which takes into account finite-size particle effects and spatial grid effects.

Although the fluctuation amplitude due to round-off errors in Fig. 4 increases with time, note that the ratio of electrostatic energy to thermal energy,  $[(eE/m_e \omega_p)^2 / v_t^2]$ , at  $t = 0$  is  $4.25 \times 10^{-6}$  in this simulation. Particle simulation with such good quality, at such a low electrostatic energy level, has not been feasible with previous models. For example, in order to reduce the fluctuation level to  $10^{-6}$  times the thermal energy in a particle simulation with the same system length, it would require  $10^3 - 10^4$  times more particles than are used in this simulation. Since the computing cost increases roughly in proportion to the number of particles, it would be prohibitively expensive. In contrast, the computing cost in this simulation was found to be less than twice that with the corresponding CIC model. Suppose the smoothing operation is performed every

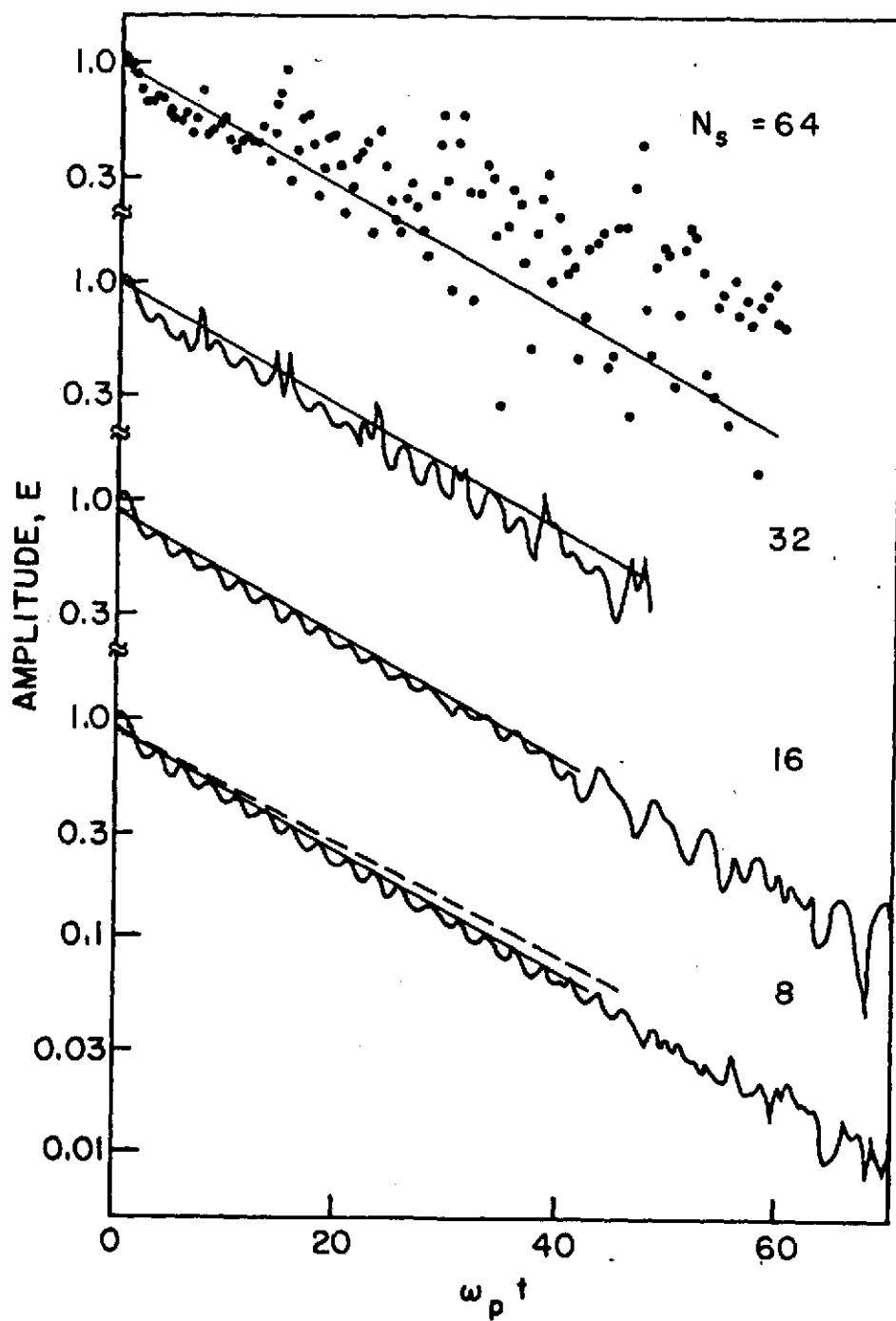


FIG. 4. Simulation of Landau damping. Solid lines are the prediction of the Langdon theory.<sup>6</sup> Dashed line is the prediction of point particle theory.

16 time-steps. One smoothing operation in our computer code takes about 7 sec on an IBM 360/67 for 8192 particles. It is equivalent to an increase of about 0.44 sec per time-step. Since it takes our computer code about 0.75 sec per time-step for the CIC model with 8192 particles and a system with 128 cells, the total computing time per time-step is about 1.2 sec.

In addition to our check on temporal Landau damping of a signal, we have verified the predicted linear dispersion characteristics of electron plasma waves. The results are shown in Fig. 5, and agree well with theory. The initial perturbations were applied for Modes 7-20 with random phases. The electrostatic energy of the individual modes excited was about  $4 \times 10^{-6}$  times the thermal energy at  $t = 0$ .

The simulation results presented in this section serve to demonstrate that the hybrid approach provides quantitatively accurate results on the collective behavior of plasma in the linear régime, where comparison with theory can readily be made. There is no reason why it should not be an equally effective tool in the nonlinear régime, for which analytical results are not so readily available. In the remainder of the paper, we shall employ it in the study of a number of nonlinear wave phenomena which appear when the signal amplitude is increased. Before doing so, however, we may comment on a well-known phenomenon associated with simulation by the Vlasov equation approach.

#### 4.1 Recurrence Phenomenon

In a simulation such as that carried out in this section, a perturbation with wavenumber  $k$  first damps to a low level at the Landau damping rate, and then reappears suddenly at time  $t = 2\pi/k\Delta v$  with higher

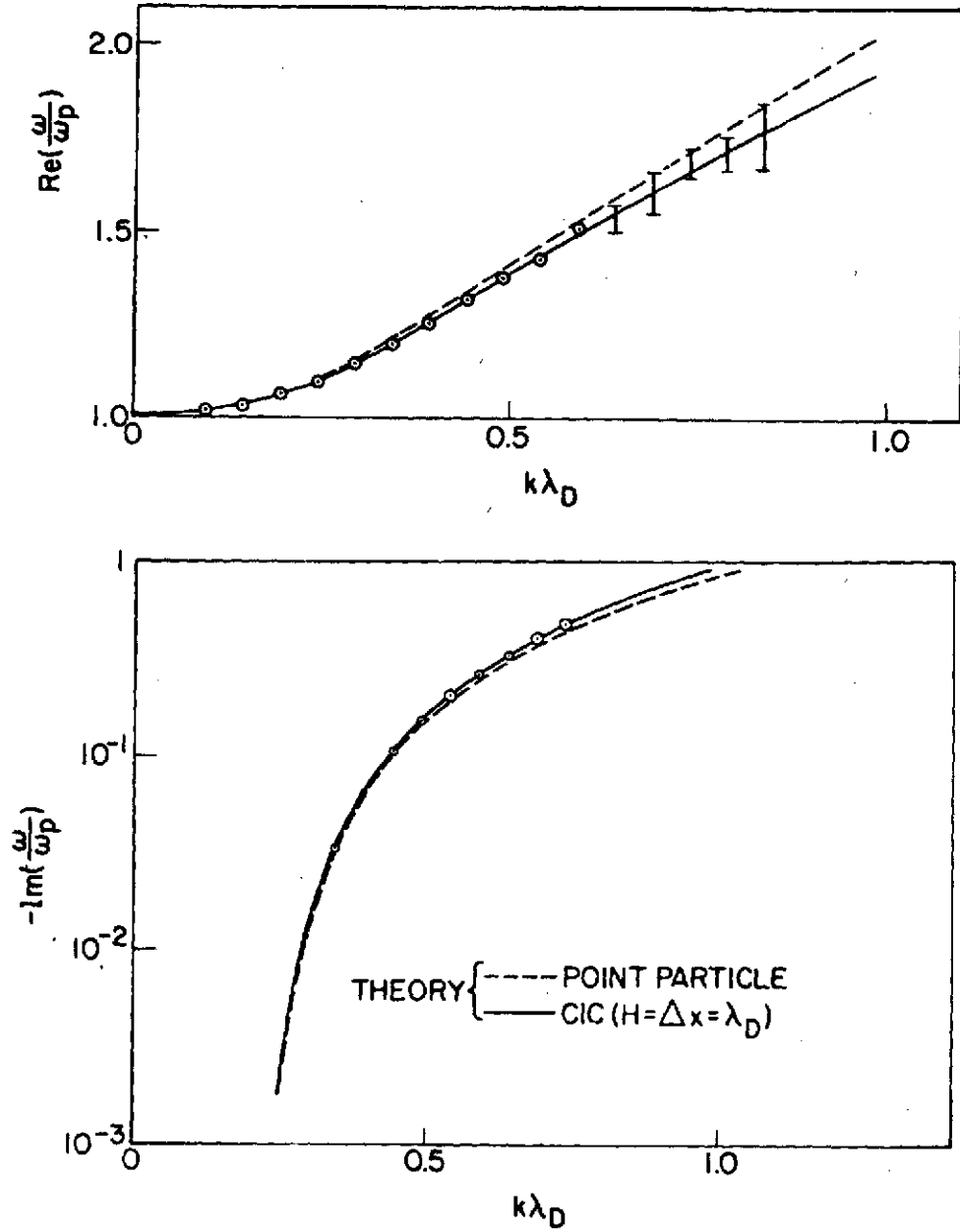


FIG. 5. Linear wave dispersion. Simulation results are shown by circles and bars whose sizes indicate errors involved. [ $\Delta v = v_t/7$ ,  $N_s = 16$ ,  $N = 8192$ ,  $L = 128 \Delta x$ ,  $v_1 = -4.5 v_t$ ,  $v_2 = 4.5 v_t$ ,  $\Delta t = 0.25/\omega_p$ ].

amplitude than its initial one. After its reappearance, the perturbation decays with a damping rate slightly different from the Landau damping rate. This recurrence results from approximating the continuous distribution function by a finite number of delta-function beams: the perturbation with wavenumber  $k$  on each beam comes back into phase after a time  $\tau_R = 2\pi/k\Delta v$ , and with larger amplitude than its initial value due to the streaming instability. In the limit of infinitely many beams, phase-mixing prevents recurrence of the initial state. The recurrence phenomenon was observed by Denavit.<sup>1</sup> Similar phenomena have been observed in the numerical solution of the Vlasov equation by the Fourier-Hermite method,<sup>11</sup> the finite difference method,<sup>11</sup> and the Lewis variational method,<sup>12</sup> and have been ascribed to finite resolution in describing velocity-space oscillations. According to our own numerical experiments, periodic smoothing alone does not suffice to prevent the recurrence.

In anticipation of succeeding sections on nonlinear phenomena, we can say that the recurrence phenomenon has not been found to pose any problems in our simulations. In Section 5, on large amplitude wave propagation, no irregularity is demonstrated at the recurrence time,  $\tau_R$ . Similarly, where growth of small amplitude test waves is concerned, no irregularity is observed.

## 5. NONLINEAR WAVE PROPAGATION

Since plasma is a highly nonlinear medium, the linearized analysis gives only a limited description of its behavior. The question arises of what will happen to Landau damping and wave dispersion when the wave amplitude is increased. Theoretical studies of this question were first made by O'Neil,<sup>13</sup> and Al'tshul and Karpman.<sup>14</sup> These authors found that the amplitude changes in time in an oscillatory manner, after initial Landau damping. The amplitude oscillation is due to periodic exchange of energy between the wave and electrons trapped in the potential wells of the wave. The exchange occurs on a time scale of  $1/\omega_B$ , where  $\omega_B [= (ekE_0/m_e)^{1/2}]$  is the bounce frequency of an electron oscillating at the bottom of a potential well,  $k$  is the wavenumber, and  $E_0$  is the wave electric field amplitude.

In solving the Vlasov equation, O'Neil, and Al'tshul and Karpman, assumed that the amplitude variation is so small as to satisfy  $\gamma_L/\omega_B \ll 1$ , where  $\gamma_L$  is the Landau damping rate. Under the same assumption, Bailey and Denavit have taken into account the effects of the slowly-varying amplitude, and obtained essentially the same amplitude oscillation, except that the time at which the amplitude begins to grow again after the initial damping is delayed.<sup>15</sup> Gary has treated the case  $\gamma_L/\omega_B > 1$  analytically, and shown that the wave starts to decay at a rate smaller than the Landau damping rate at a time when the linear theory is expected to break down.<sup>16</sup> Sugihara and Kamimura have considered a wide range of  $\gamma_L/\omega_B$  values. Unlike the theories mentioned so far, their treatment is self-consistent: it includes the interaction

between the electric field and the averaged electron velocity distribution.<sup>17</sup> Recent work by Oei and Swanson is also self-consistent, and gives similar results to those of Sugihara and Kamimura for  $0 < \gamma_L/\omega_B \lesssim 1$ .<sup>18</sup>

All of the theoretical studies discussed above assume that the electric field is so small that the distribution function in the resonant region can be expressed by a Taylor expansion about the wave phase velocity up to the first order term in velocity. This condition may be written as  $\omega/\omega_B \gg (v_p/v_t)^2$ , where  $v_p$  is the phase velocity of the wave ( $\omega/k$ ). This is such a stringent condition that it is not easy to meet in laboratory experiments, especially when also satisfying the condition  $\gamma_L/\omega_B \ll 1$ .

A few experimental data on Landau damping of large amplitude waves have been reported. Malmberg and Wharton<sup>19</sup> observed spatial amplitude oscillation in qualitative agreement with the O'Neil theory<sup>13</sup> modified to fit the spatial case by Lee and Schmidt.<sup>20</sup> Oei and Swanson compared their theoretical results with the experiments of Malmberg and Wharton, and found agreement on the amplitude oscillation lengths but not on the detailed behavior of the amplitude.<sup>18</sup> One of the reasons may be that their experimental parameters do not meet the condition  $\omega/\omega_B \gg (v_p/v_t)^2$ . Specifically, they have  $\gamma_L/\omega_B \sim 0.1$  and  $\omega/\omega_B \sim (v_p/v_t)^2$  for the results which exhibit amplitude oscillation. Franklin et al. have made detailed measurements of the spatial dependence of amplitude for electron plasma waves with different initial amplitudes, i.e., for different values of  $\omega_B$ .<sup>21</sup> However, for large initial amplitude, they failed to obtain results in agreement with the theory. This was ascribed to the appearance of sideband growth due to trapped particle instability.<sup>22</sup> Their experimental parameters for the measured results, corresponding to  $\gamma_L/\omega_B \lesssim 0.45$ , yield  $\omega/\omega_B \lesssim 4(v_p/v_t)^2$ .



This suggests that comparison of the available theories with the experiments is inappropriate.

In view of the foregoing difficulties, computer simulation suggests itself as a means of bridging the gap between the theoretical assumptions and readily attainable experimental parameters. It allows conditions to be studied for which analytical approaches are not tractable. Such simulations have been carried out by Knorr,<sup>23</sup> and Armstrong,<sup>24</sup> using direct solution of the Vlasov equation, and by Dawson and Shanny,<sup>25</sup> using the particle simulation model. Knorr observed a decrease in the damping rate for large amplitude waves at times such that  $\omega_B t \sim 1$ . Armstrong considered the same problem and found in addition to Knorr's results that large amplitude waves grow again after damping initially. He also found that the initial damping of a large amplitude wave is stronger than is predicted by the Landau theory. A similar observation of the enhanced initial damping was made by Dawson and Shanny.

One of our purposes has been to use the hybrid model described in Section 2 to investigate the nonlinear behavior of longitudinal monochromatic plasma waves more comprehensively than has been possible previously. Another has been to investigate the nonlinear frequency shift of electron plasma waves. In a plasma of infinite extent, or of finite length with periodic boundary conditions, the frequency of a wave of large amplitude deviates from that of a small amplitude wave due to nonlinear effects. In an experimental plasma, in which a wave is excited at a fixed frequency, the shift should occur in wavelength instead of frequency.

The frequency shift has been studied analytically by Manheimer and Flynn,<sup>26</sup> Morales and O'Neil,<sup>27</sup> Dewar,<sup>28</sup> and Lee and Pocobelli,<sup>29</sup> and found

to be proportional to  $E_0^{1/2}$ . So far, there has been no report of laboratory observations of nonlinear wavelength shift for comparison with these theories. In this section, we shall test the theoretical predictions of nonlinear frequency shift against computer simulations carried out by use of the hybrid model.

### 5.1 Computations

We have performed a series of computer simulations to demonstrate the nonlinear behavior of monochromatic electron plasma waves in a collisionless plasma. The electrostatic energy of the waves in these simulations was of the order of  $10^{-4}$  times the thermal energy. This is about two orders of magnitude smaller than in the simulations of Dawson and Shanny.<sup>25</sup> Some of the simulations by Knorr,<sup>23</sup> and Armstrong,<sup>24</sup> are in our range of energy. Their computations have not, however, been carried out for long enough times to demonstrate amplitude oscillation.

Amplitude Oscillation: Figure 6 demonstrates clearly this phenomenon. Mode 3 was excited initially according to Eq. (3), and the evolution of the amplitude was followed in time with periodic boundary conditions applied in space. The amplitude oscillates and approaches a constant value due to phase-mixing of the trapped particles, and formation of a Bernstein-Green-Kruskal (BGK) mode.<sup>30</sup>

The initial amplitude of the wave was  $eE_0/m_e v_t \omega_p \simeq 3.4 \times 10^{-2}$ , corresponding to a bounce frequency of  $\omega_B/\omega_p \simeq 0.09$ . The measured initial damping rate is  $\gamma_L/\omega_p \simeq 0.0119$ . These combine to give  $\gamma_L/\omega_B \simeq 0.13$ . The measured frequency is  $\omega/\omega_p \simeq 1.15$ . The corresponding wave phase velocity is  $v_p/v_t \simeq 3.91$ , so that  $\omega/\omega_B \simeq 13$  and  $(v_p/v_t)^2 \simeq 15$  are of the same order.

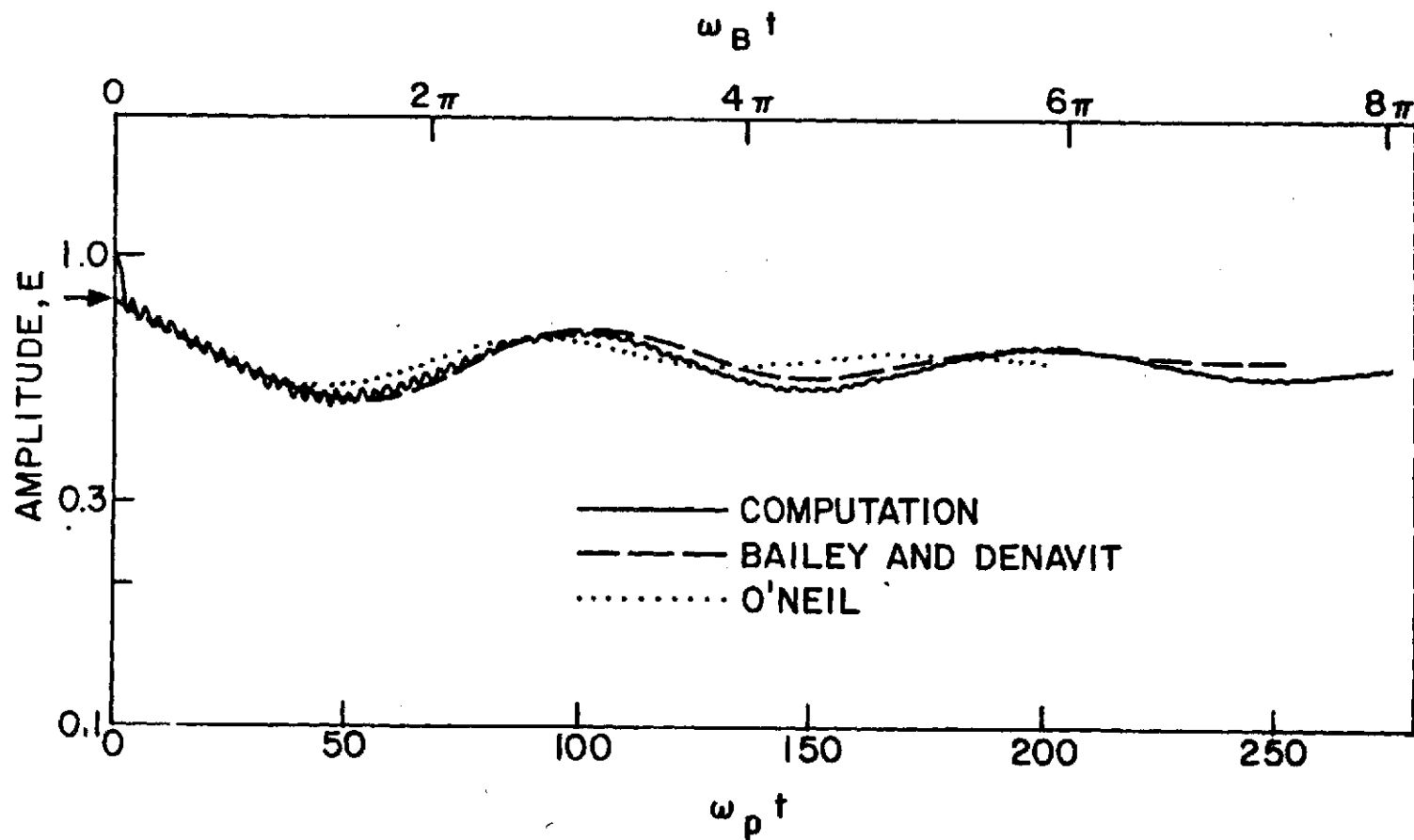


FIG. 6. Amplitude oscillation of a large amplitude monochromatic wave. [ $\Delta v = v_t/14$ ,  $N_s = 16$ ,  $N = 8192$ ,  $L = 64 \Delta x$ ,  $H = \Delta x = \lambda_D$ ,  $v_1 = -4.25 v_t$ ,  $v_2 = 4.82 v_t$ ,  $\Delta t = 0.25/\omega_p$ ].  
(Nonsymmetric velocity-space is used to provide resonant particles at high velocities.)

Figure 7 shows the temporal behavior of the distribution function, in the vicinity of the wave phase velocity, averaged over space. The changes in the distribution are relatively small; for example, at  $\omega_p t = 48$ , the ratio of the peak value to the maximum value of the (nearly) Maxwellian distribution is of the order of  $10^{-3}$ . A bump is formed in the distribution for  $\omega_p t \simeq 48$ , and reappears for  $\omega_p t \simeq 144$  and  $240$ . Comparison with Fig. 6 indicates that these times correspond approximately to minima in the amplitude. The height of the bump becomes progressively smaller on its reappearances, because of phase-mixing of the trapped particles.<sup>13</sup> A similar bump was observed by Armstrong, and considered to cause growth of waves with phase velocities lying in that region of the bump that has positive slope.<sup>24</sup> The bump on the tail of the distribution function has spatial structure. This may be contrasted with the initially spatially homogeneous distribution whose evolution is considered in the quasilinear theory of a warm beam-plasma system.<sup>31,32</sup>

In Fig. 8, we present the results of a series of simulations for various values of the initial electric field,  $E_0$ , expressed in terms of the convenient parameter  $\gamma_L/\omega_B$ , where we recall that  $\omega_B = (ekE_0/m_e)^{1/2}$ . Only one mode was excited at  $t = 0$  for each simulation run, and a different mode and amplitude were used in each run. The amplitude was normalized to unity at  $t = 0$  in the plots. It will be seen from Fig. 8 that amplitude oscillation occurs for small values of  $\gamma_L/\omega_B$ , and that the oscillation becomes less pronounced, with Landau damping extended for a longer period, as  $\gamma_L/\omega_B$  increases. The fluctuations in the curves for large values of  $\gamma_L/\omega_B$  are due to the round-off errors made in representing numbers by a finite number of digits in the computer.

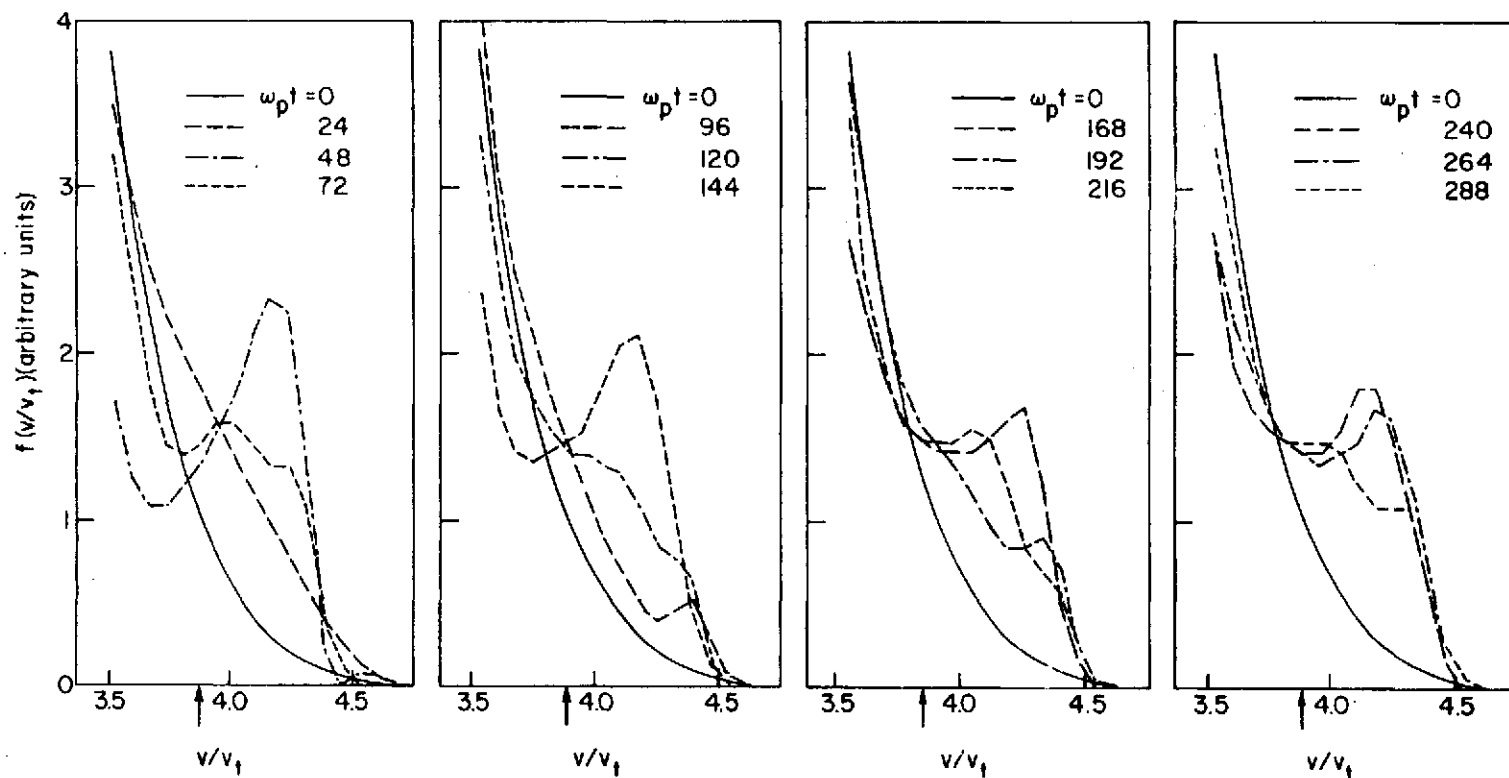


FIG. 7. Temporal behavior of the spatially-averaged distribution function in the simulation shown in Fig. 6. The phase velocity of the wave is marked by an arrow.

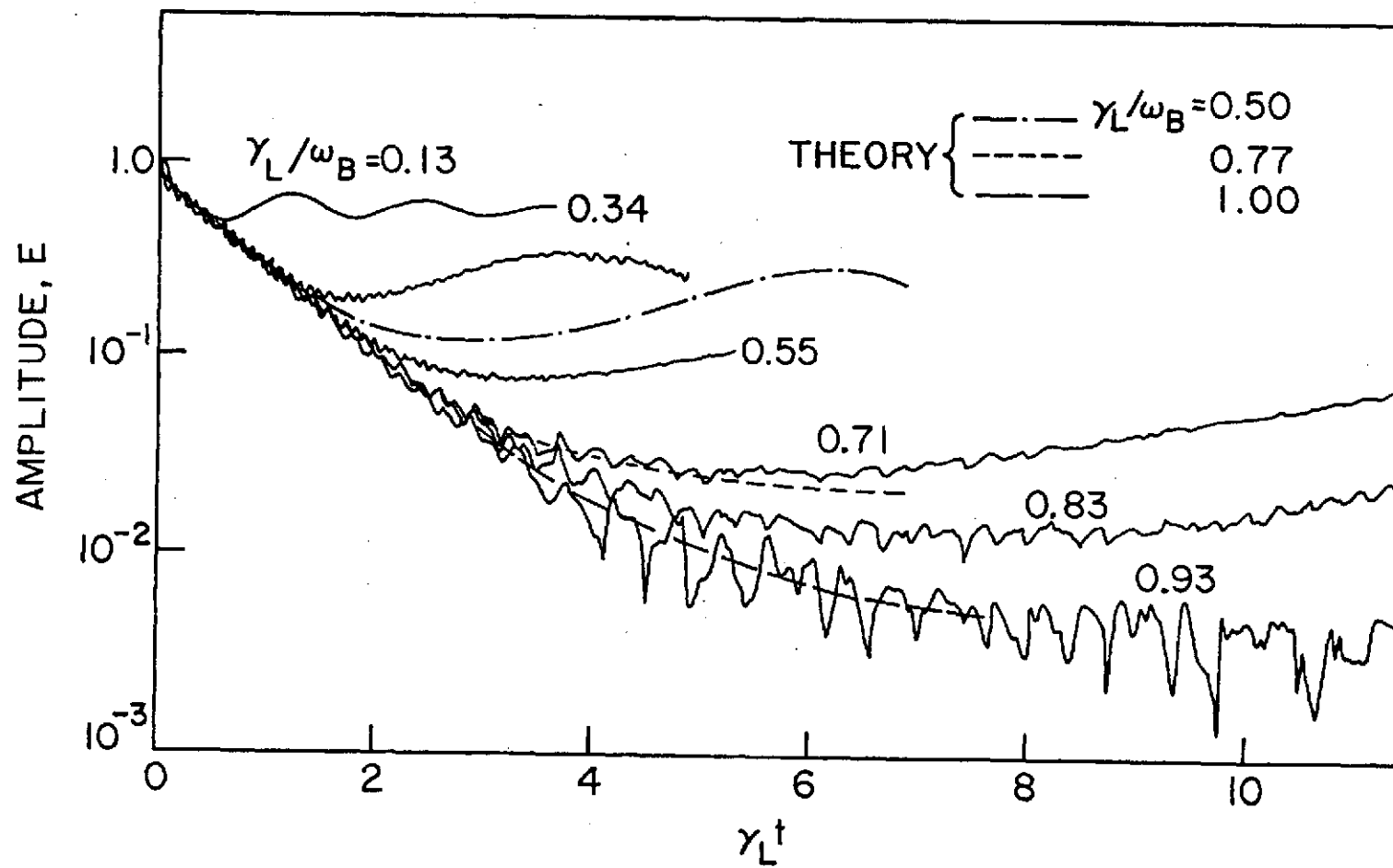


FIG. 8. Temporal evolution of amplitude for various initial amplitudes, i.e.,  $\gamma_L / \omega_B$ .

Frequency Shift: Figure 9 shows the variation of the nonlinear frequency shift as a function of the electric field amplitude. Mode 3 was excited initially according to Eq. (3), with amplitude  $(eE_0/m_e v_{te} \omega_p)$  varying from small values ( $9 \times 10^{-3}$ ), which exhibit Landau damping, to large values ( $3 \times 10^{-1}$ ) such as were studied in the simulations of Dawson and Shanny.<sup>25</sup> For each simulation with different amplitude, the frequency of Mode 3 was measured by computing the total amount of phase change in the Fourier transform of the electric field between  $\omega_p t = 6$  and 60. The frequency shift plotted in Fig. 9 was then obtained by subtracting the linear frequency,  $\omega_L = 1.247 \omega_p$ , obtained from the Langdon theory,<sup>6</sup> from the measured frequency. Except for very small amplitudes, the nonlinear frequency shift is proportional to  $E_0^{1/2}$ , and given by

$$\frac{\delta\omega}{\omega_p} = 0.006 - 0.2 \frac{\omega_B}{\omega_p} \quad (4)$$

To check the dependence of this result on the beam spacing, the simulations were repeated with the beam spacing halved, and the same number of smoothing operations. The differences in frequency shift were not more than 3%.

A significant fact to note here is the high degree of accuracy with which it was possible to determine the frequency, and frequency shift. The model based on the hybrid approach is, therefore, much more efficient than a particle code in terms of computing cost for this measurement.

## 5.2 Comparison with Theory

First, we may check the observed initial damping against the linear theory of Langdon,<sup>6</sup> which includes finite size particle and spatial grid effects. The theoretical values of the Landau damping rate,  $\gamma_L$ , and

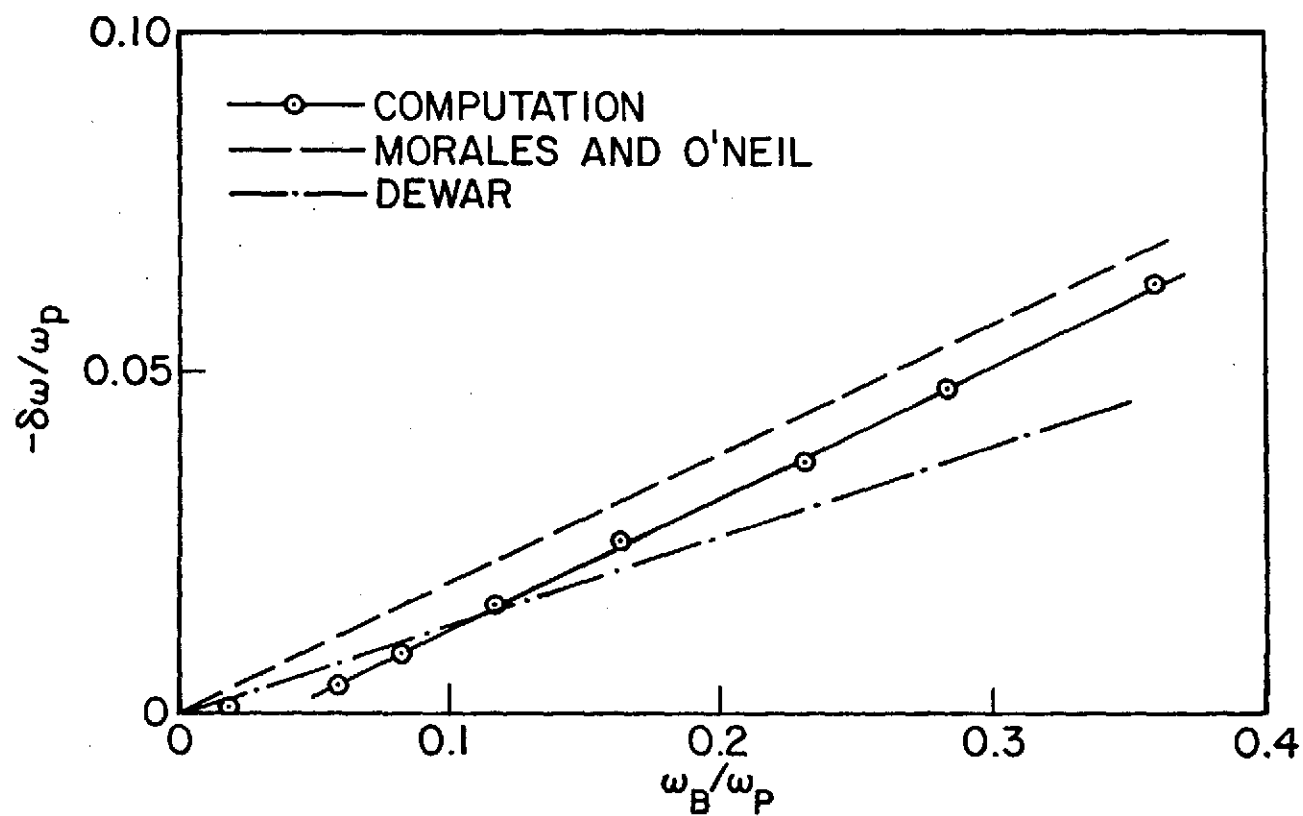


FIG. 9. Nonlinear frequency shift of an electron plasma wave. [ $\Delta v = v_t/7$ ,  $N_s = 16$ ,  $N = 4096$ ,  $L = 50 \lambda_D$ ,  $H = \Delta x = (50/64)\lambda_D$ ,  $v_1 = -3.79 v_t$ ,  $v_2 = 5.21 v_t$ ,  $\Delta t = 0.25/\omega_p$ ].



frequency,  $\omega_L$ , obtained by retaining only the  $p = 0$  term in the summation in the expression for plasma permittivity given in Reference 6 are  $\gamma_L/\omega_p = 0.0118$  and  $\omega_L/\omega_p = 1.145$  for Mode 3 plotted in Fig. 6. We see very good agreement with the measurements described in Section 5.1. The theoretical predictions for each mode presented in Fig. 8 have also been found to agree with the measured initial damping and frequency with errors of less than 1%.

Amplitude Oscillation: Next we consider the nonlinear theories due to O'Neil,<sup>13</sup> Bailey and Denavit,<sup>15</sup> and Sugihara and Kamimura.<sup>17</sup> O'Neil obtained a theoretical expression for the time-varying damping rate by using an energy conservation relation between the resonant particles and the wave. Substituting the initial damping rate ( $\gamma_L/\omega_B = 0.0119$ ) obtained from our computer simulation (Fig. 6), and the bounce frequency ( $\omega_B/\omega_p = 0.09$ ) calculated from the initial amplitude in the same simulation, we obtain the amplitude variation plotted in Fig. 6. After damping initially, the wave starts to grow somewhat earlier than it does in the simulation. This can be ascribed to the variation in wave amplitude, which was not taken into account in calculating particle trajectories.

Bailey and Denavit incorporated the effects of slowly-varying wave amplitude to lowest order in  $\dot{\alpha}/\alpha^2$ , where  $\alpha(t) = [ekE(t)/m_e]^{1/2}$ ,  $\omega_B = \alpha(0)$ , and  $\dot{\alpha} = d\alpha/dt$ . We have solved numerically a set of differential equations which they obtained, for the same values of  $\gamma_L$  and  $\omega_B$  used above, and with the results plotted in Fig. 6. There is very good agreement between the theory and the simulation. We note, however, that there is a slight difference in amplitude, and that the phase-mixing is somewhat slower in the

simulation results than the theory predicts. These differences are probably due, first, to the fact that the condition,  $\omega/\omega_B \gg (v_p/v_t)^2$ , is not satisfied in the simulation, and second, that the theory of Bailey and Denavit is not self-consistent.

Sugihara and Kamimura derived from the Vlasov equation a set of integro-differential equations which describe the behavior of the amplitude of a monochromatic wave. Numerical solutions of these integro-differential equations demonstrated amplitude oscillation for  $\gamma_L/\omega_B \ll 1$ , and Landau damping for  $\gamma_L/\omega_B \gg 1$ . Some of their results are reproduced in Fig. 8. First, we note that their calculation shows that, for  $\gamma_L/\omega_B = 0.1$ , the amplitude approaches a constant value after nearly two periods of oscillation, although the distribution function still retains nonuniform features. In our simulation, however, the amplitude oscillation lasts more than two periods, and does not seem to die out so quickly. This fact seems to be in at least qualitative agreement with a nonlinear spatial Landau damping experiment by Malmberg and Wharton<sup>19</sup> in which there was no clear sign of phase-mixing. A similar feature of this persistent amplitude oscillation was also observed in the behavior of an externally excited large amplitude wave in a simulation of sideband instability by Denavit and Kruer.<sup>9</sup> Second, we recall that Sugihara and Kamimura found that there is a critical value of  $\gamma_L/\omega_B = 0.77$ , which separates waves into those with oscillatory behavior ( $\gamma_L/\omega_B < 0.77$ ), and those which are continuously damped ( $\gamma_L/\omega_B > 0.77$ ). Figure 8 indicates that there is no such critical value below  $\gamma_L/\omega_B = 0.93$ . Third, we note that there is a tendency in our simulation results for the amplitude to decrease to a lower level, for a given value of  $\gamma_L/\omega_B$ , than is predicted by the theory of Sugihara and Kamimura; the first maximum is also lower than

the theory predicts. Although the simulation results given in Fig. 8 are similar to the theoretical results obtained by Sugihara and Kamimura, it is important to note that in our simulations  $\omega/\omega_B \gtrsim (v_p/v_t)^2$ , whereas they implicitly assumed that  $\omega/\omega_B \gg (v_p/v_t)^2$ .

Frequency Shift: Manheimer and Flynn<sup>26</sup> examined the self-consistency of the O'Neil solution for the time-asymptotic state:<sup>13</sup> they studied whether the potential created by the O'Neil solution satisfies the Poisson equation. They found that it is approximately self-consistent if a frequency shift given by

$$\delta\omega = -\beta \left( \frac{eE_0}{m_e k} \right)^{1/2} \left( \frac{\omega^2}{k^2} \right) \left( \frac{\partial^2 f_0}{\partial v^2} \right)_{v=v_p} \left( \frac{\partial \epsilon_p}{\partial \omega} \right)^{-1}_{\omega=\omega_L}, \quad (5)$$

is included, where  $\beta$  is a numerical factor equal to  $2^{1/2}$ ,  $f_0$  is the initial distribution function, and  $\epsilon_p$  is the linear plasma permittivity. In deriving Eq. (5), Manheimer and Flynn only considered the trapped particles with simple harmonic motions, i.e., those near the potential wells of the wave, and the untrapped particles with straight line orbits. Morales and O'Neil solved an initial value problem to find the time-dependent shift in the complex frequency of the wave.<sup>27</sup> They took into account the exact trajectories for both the trapped and untrapped particles, and obtained a frequency shift which varies in an oscillatory manner and approaches a constant value in the time-asymptotic limit. Their time-asymptotic frequency shift is expressed in the same form as Eq. (5) except that  $\beta \approx 1.63$ .

Lee and Pocobelli predicted frequency shifts for waves with  $v_p/v_t \gtrsim 4$  up to about 50% larger than those predicted by Morales and O'Neil. These were obtained by including effects of electrons not in the vicinity of the

phase velocity of the wave.<sup>29</sup> In contrast to these theories treating the case in which the wave is switched on suddenly at  $t = 0$ , Dewar considered the case of an adiabatically excited wave, i.e., the wave was turned on gradually.<sup>28</sup> He obtained a time-asymptotic frequency shift similar to that expressed by Eq. (5), but with  $\beta = 1.09$ .

Substituting  $\omega_L/\omega_p = 1.247$  for Mode 3, obtained from the Langdon theory and the Maxwellian distribution for  $f_0$  in Eq. (5), we have

$$\delta\omega \simeq \begin{cases} -0.19\omega_B & \text{(Morales and O'Neil),} \\ -0.13\omega_B & \text{(Dewar) ,} \end{cases} \quad (6)$$

which are plotted in Fig. 9. We see that the slopes of the lines from the simulation, and from the theory of Morales and O'Neil, are very similar. This is to be expected because our simulation of an initial value problem resembles the Morales and O'Neil problem, rather than the Dewar problem. It should be remembered, however, that the theoretical result is the time-asymptotic value, whereas the measured frequency shift is an average over the period  $\omega_p t = 6$  to  $60$ . It should also be recalled that the value of  $\omega_B$  corresponds to the initial amplitude of the wave. Since the theoretical result due to Morales and O'Neil was obtained under the condition that the amplitude variation is very small, it does not matter much whether the bounce frequency is computed from the initial amplitude or from the time-asymptotic amplitude. In our simulation, however, the amplitude variation is not negligible; if the bounce frequency were computed from the time-asymptotic amplitudes, the points in Fig. 9 would be moved towards the

theoretical line of Morales and O'Neil. A similar amplitude dependence of the nonlinear frequency shift has recently been observed using the Vlasov approach.<sup>33</sup>

Lee and Pocobelli have reported further simulation results of nonlinear frequency shift.<sup>34</sup> They used a one-dimensional particle simulation model (charge sheet model) with a spatial grid, and obtained agreement between measured frequency shifts and theoretical calculations.<sup>28</sup> In this simulation, a standing wave was driven by applying external electric field for a short time. This is in contrast to our case of an initial value problem with a propagating wave. It is noteworthy that they used as many as 40,000 particles. We needed only 4096 particles to obtain quantitative results of similar quality using the hybrid model.

## 6. DISCUSSION

In this part of our paper, we have studied essentially monochromatic electron plasma wave propagation by means of a variant of the economical, low-noise, hybrid simulation approach of Denavit.<sup>1</sup> In Sections 3 and 4, computational studies of the model were made for equilibrium conditions, and small-signal propagation. The linear wave dispersion characteristics predicted by theory for long wavelength collective behavior were demonstrated to be followed very precisely. This verification of the validity and effectiveness of the simulation model is very important as a starting point for the subsequent study of nonlinear phenomena. It also serves to establish the validity of the widely-used CIC model,<sup>2</sup> and the Langdon theory describing the finite-size particle model.<sup>6</sup> Quantitative results in the very low energy range discussed here have never been obtained previously with such a high degree of accuracy with simple particle models.

In the study of amplitude oscillation and Landau damping in Section 5, we have attempted investigation in areas where analytical approaches are not easily tractable, i.e., in cases where the condition,  $\omega/\omega_B \gg (v_p/v_t)^2$ , is not satisfied. The results of our simulations show good qualitative agreement with the theories of Bailey and Denavit,<sup>15</sup> and Sugihara and Kamimura,<sup>17</sup> who have made the assumption,  $\omega/\omega_B \gg (v_p/v_t)^2$ . However, there are significant differences between our simulation results and the theoretical results of these authors; first, phase-mixing of the amplitude oscillation is slower than predicted, and second, there exists no critical

value of  $\gamma_L/\omega_B$  within our parameter range such as was found by Sugihara and Kamimura. It is hoped that these results will be helpful in better understanding the phenomenon, and in developing an analytical theory for  $\omega/\omega_B \lesssim (v_p/v_t)^2$ .

In the study of nonlinear frequency shift made in Section 5, we have measured the frequency shift for large amplitude waves, and compared the results with theoretical predictions. It has been demonstrated that the simulation results agree well with the theoretical predictions of Morales and O'Neil.<sup>27</sup>

The deformation of the velocity distribution, particularly particle trapping, caused by a large-amplitude wave gives rise to a variety of wave amplification and coupling phenomena. Sidebands develop in addition to the monochromatic wave applied, and additional satellite frequencies appear. These can be studied as growth from noise, or by injection of suitable test waves. A series of such studies is presented in Part II of the paper.<sup>35</sup>

## REFERENCES

1. J. Denavit, J. Comp. Phys. 2, 75 (1972).
2. C. K. Birdsall and D. Fuss, J. Comp. Phys. 3, 494 (1969).
3. J. A. Byers, Proc. Fourth Conference on Numerical Simulation,  
November 1970, Naval Research Laboratory, Washington, D. C., p. 496.
4. J. M. Dawson, Phys. Rev. 118, 381 (1960).
5. H. R. Lewis, in Methods in Computational Physics, edited by  
B. Alder, S. Fernbach, and M. Rotenberg (Academic Press, New York,  
N. Y., 1970), Vol. 9, p. 307.
6. A. B. Langdon, J. Comp. Phys. 6, 247 (1970).
7. R. L. Morse and C. W. Nielson, Phys. Fluids 12, 2418 (1969).
8. T. P. Armstrong and C. W. Nielson, Phys. Fluids 13, 1880 (1970).
9. J. Denavit and W. L. Kruer, Phys. Fluids 14, 1782 (1971).
10. Y. Matsuda, Stanford University Institute for Plasma Research Report  
No. 567 (March 1974).
11. J. Canosa and J. Gazdag, Proc. Sixth Conference on Numerical Simulation  
of Plasmas, July 1973, Lawrence Livermore Laboratory Report No. CONF-  
730804, Berkeley, California, p. 104.
12. H. R. Lewis, Phys. Fluids 15, 103 (1972).
13. T. M. O'Neil, Phys. Fluids 8, 2255 (1965).
14. L. M. Al'tshul and V. I. Karpman, Sov. Phys. JETP 22, 361 (1966).
15. V. L. Bailey and J. Denavit, Phys. Fluids 13, 451 (1970).
16. S. P. Gary, Phys. Fluids 10, 570 (1967).
17. R. Sugihara and T. Kamimura, J. Phys. Soc. Japan 33, 206 (1972).
18. I. H. Oei and D. G. Swanson, Phys. Fluids 15, 2218 (1972).



19. J. H. Malmberg and C. B. Wharton, Phys. Rev. Letters 19, 775 (1967).
20. A. Lee and G. Schmidt, Phys. Fluids 13, 2546 (1970).
21. R. N. Franklin, S. M. Hamberger, and G. J. Smith, Phys. Rev. Letters 29, 914 (1972).
22. W. L. Kruer, J. M. Dawson, and R. N. Sudan, Phys. Rev. Letters 23, 838 (1969).
23. G. Knorr, Z. Naturforsch. 18a, 1304 (1963).
24. T. P. Armstrong, Phys. Fluids 10, 1269 (1967).
25. J. M. Dawson and R. Shanny, Phys. Fluids 11, 1506 (1968).
26. W. M. Manheimer and R. W. Flynn, Phys. Fluids 14, 2393 (1971).
27. G. J. Morales and T. M. O'Neil, Phys. Rev. Letters 28, 417 (1972).
28. R. L. Dewar, Phys. Fluids 15, 712 (1972).
29. A. Lee and G. Pocobelli, Phys. Fluids 15, 2351 (1972).
30. I. B. Bernstein, J. M. Green, and M. D. Kruskal, Phys. Rev. 108, 546 (1957).
31. W. E. Drummond and D. Pines, Nucl. Fusion Suppl. Pt. 3, 1049 (1962).
32. A. A. Vedenov, E. P. Velikhov, and R. Z. Sagdeev, Nucl. Fusion Suppl. Pt. 2, 465 (1962).
33. J. Canosa, private communication.
34. A. Lee and G. Pocobelli, Phys. Fluids 16, 1964 (1973).
35. Y. Matsuda and F. W. Crawford, Phys. Fluids [= Part II of the paper].